Theoretical modelling of momentum transfer function of bi-disperse porous media

K. Hooman [a, *], E. Sauret [b], M. Dahari [c]

[a] School of Mechanical and Mining Engineering, The University of Queensland, Qld 4072, Australia
[b] School of Chemistry, Physics & Mechanical Engineering, Queensland University of Technology, Qld 4000, Australia
[c] Department of Mechanical Engineering, Faculty of Engineering, University of Malaya, 50603 Kuala Lumpur, Malaysia

HIGHLIGHTS

- Test results for a designed bi-disperse porous medium are investigated and analysed.
- N–K model is applied to analyse the results for a range of fluid velocity and geometry.
- Drag coefficient is obtained as a function of pertinent parameters.

GRAPHICAL ABSTRACT

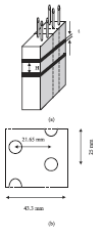

ARTICLE INFO

Article history:
Received 3 August 2014
Accepted 7 October 2014
Available online 30 October 2014

Keywords:
Bi-disperse
Porous media
Drag

ABSTRACT

The aim of this paper is to obtain the momentum transfer coefficient between the two phases, denoted by f and p, occupying a bi-disperse porous medium by mapping the available experimental data to the theoretical model proposed by Nield and Kuznetsov [1]. Data pertinent to plate-fin heat exchangers, as bi-disperse porous media, were used. The measured pressure drops for such heat exchangers are then used to give the overall permeability which is linked to the porosity and permeability of each phase as well as the interfacial momentum transfer coefficient between the two phases. Accordingly, numerical values are obtained for the momentum transfer coefficient for three different fin spacing values considered in the heat exchanger experiments.

1. Introduction

Chen et al. [2] tested a bidisperse porous medium (BDPM), clusters of large particles which, in turn, are agglomerations of small particles, with very high area to volume ratios to note interesting thermal conductivity behaviour. As such, engineering applications for BDPMs such as bidisperse adsorbent or wicks and evaporators in heat pipes are mentioned on top of biological structures, such as bone regeneration scaffolds; also characterized by bimodal pore distributions [3–5]. Coal stockpiles can be mentioned as other examples [6–8]. Such stockpiles are formed by piling (usually) small coal particles which are porous themselves. The stockpile porosity is usually higher than that of particles. Self-heating of such stockpiles is a significant challenge addressing which calls for a deep understanding of flow behaviour at both particle and inter-particle levels. Nield and Kuznetsov [1] suggested a theoretical model to relate the overall permeability to that of individual phases. According to those authors, two phases are defined being the f-phase (the macropores) and the p-phase (the remainder of the structure). The pressure drop is then modelled as the superposition of Darcy resistance for each phase and an interfacial momentum exchange which is linearly proportional to the

* Corresponding author. Tel.: +61 7 33653677; fax: +61 7 33654799.
E-mail address: k.hooman@uq.edu.au (K. Hooman).

http://dx.doi.org/10.1016/j.applthermaleng.2014.10.067
1359-4311/

velocity difference between the two phases as well as an interfacial momentum transfer coefficient. This momentum transfer coefficient, however, remains as an unknown in the literature despite the popularity of the model [9,10] and even the extensions to include shear [11] and form drag [12] effects on top of the extension to tridisperse porous materials [13]. Furthermore, the application of the model serves the basis for analysing heat transfer in BDPMs as addressed in Refs. [14–16].

Two common assumptions are made in all of the above-mentioned works. Firstly, the momentum transfer coefficient is assumed to be a homogenous constant velocity-independent value. Secondly, the numerical value of the momentum transfer coefficient is neither known nor related to porous media properties like porosity and permeability (of each phase). These both are questionable in the absence of rigorous mathematical, numerical, or experimental data. As such, the aim of this paper is to fill this gap in the literature by mapping the theoretical model developed by Ref. [1] to an experiment databank to obtain a value for the momentum transfer coefficient which could be used for future development and fine-tuning. In what follows, a brief description of the pertinent experiment is presented and the modelling assumptions are discussed along with the obtained results.

2. Analysis

In an interesting study, Kang et al. [17] reported experimental data for pressure drop and heat transfer of plate-fin heat exchanger

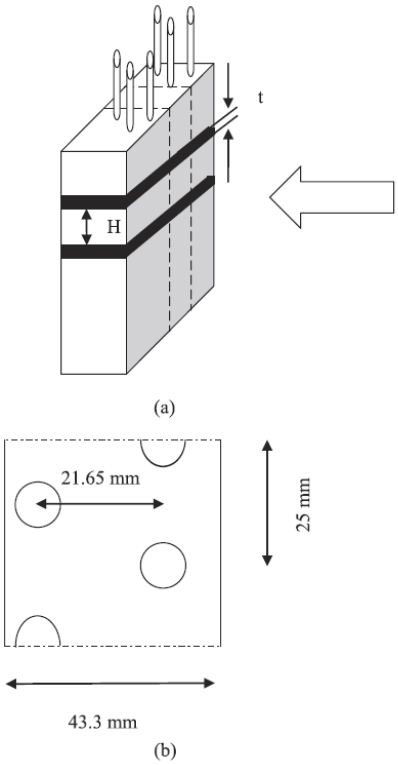

Fig. 1. Schematic description of the heat exchanger modelled as BDPM a) the heat exchanger and b) the top view of the plate.

with no intention to model the system as a porous medium. In their work, as schematically described in Fig. 1, thin plates (black parallel plates in Fig. 1) are punched to house pipes (10.55 mm diameter) through which hot water flows. Air is pushed to flow between the thin plates and cross the pipes. Air flow is normal to shaded (grey) plate in Fig. 1. In the original experiment the spacing between these plates were varied from 2, 2.6, and 3 mm to allow for different flow resistances and heat transfer. The transverse and longitudinal pitch values were not altered and the values are set as shown by Fig. 1. Here, the pipes constitute the p-phase, as separated by the dashed lines, while the spaces between parallel plates, here thick black plates, form the f-phase. The thick black plates are solid and only two of them are shown. Hot water flows in the pipe and air flows normal to the pipe in the direction shown by the arrow, e.g. a cross-flow (Forgo) heat exchanger. When the pipes are inserted, the pores of this, f-phase, porous medium are filled with another porous medium. Here, the spaces between the pipes allow for fluid flow; as such they are assumed as pores for p-phase. The permeability values for the p- and f-phase, K_p and K_f, are given in the literature [18–20] as function of porosities, pipe diameter and plate thickness as well as plate spacing. Specifically, with ε_f and ε_p denoting the porosities of f- and p-phases, d as the pipe diameter and t being the plate thickness that separates the two plates which are apart by H, one has.

$$K_p = \frac{\varepsilon_p^3 d^2}{100(1-\varepsilon_p)^2}, \tag{1}$$

$$K_f = \frac{\varepsilon_f H^2}{12}. \tag{2}$$

Development of Eq. (1) above and the extension to finned tube bundles is explained in Ref. [18] while Ref. [20] drives Eq. (2) based on flow between parallel plates. Table 1 is presented to give more details about the f- and p-phases and geometrical data taken from Ref. [17].

The overall permeability is, according to Ref. [1], given by.

$$K = \frac{\phi K_f + (1-\phi)K_p + 2(\zeta/\mu)K_f K_p}{1 + (\zeta/\mu)\left(K_f + K_p\right)}, \tag{3}$$

and is linked to the air viscosity μ and pressure gradient G as

$$G = \left(\frac{\mu}{K}\right)U^*, \tag{4}$$

where, with ϕ as the volume fraction of macropores, one has the average velocity, U^*, as

$$U^* = \phi U_f^* + (1-\phi)U_p^*. \tag{5}$$

Note that ζ in the above formulation is the unknown momentum transfer coefficient. As our goal is to obtain ζ, we rearrange Eq. (3) to get.

Table 1
Additional f- and p-phase details ($d = 10$ mm, $t = 0.2$ mm); geometrical details from [17].

H (mm)	$\varepsilon_f = 1 - \frac{t}{H}$	K_f ($\times 10^7$ m^2)	ε_p	K_p ($\times 10^5$ m^2)
3.2	0.9375	8	0.78	1.14
2.6	0.923	5.2	0.78	1.14
2	0.9	3	0.78	1.14

$$\zeta = \mu \frac{\phi K_f + (1-\phi)K_p - K}{K\left(K_f + K_p\right) - 2K_f K_p}. \tag{6}$$

Note that Eqs. (3)–(6) are taken from Ref. [1], μ is the air viscosity and our U^* range is limited to 2.5 m/s. Eq. (4) is expected to be valid for cases when the form drag effects can be neglected, i.e. when the BDPM flow resistance is dominated by the viscous drag as explained in Ref. [1]. Here, the permeability for each phase is known as a function of geometrical constrains. Similarly, ϕ is prescribed for a given geometry. One is then left to link K to ζ. We suggest the experimental results, here those in Ref. [17], be rearranged to take a form like Eq. (4) to allow for evaluation of K. Consequently, for a given geometry, ζ can be determined. In doing so, the friction factor-Reynolds correlation given by Ref. [17] is used to obtain experimental G values. Then, G/U^* is plotted against U^* and fitted with a linear distribution to give the permeability value for each experiment as shown by Fig. 2. The fitted lines are described by the following equations (for 2, 2.6, and 3.2 mm cases, respectively).

$$\frac{G}{U^*} = 23 + 150U^*, \tag{7a}$$

$$\frac{G}{U^*} = 15.5 + 110U^*, \tag{7-b}$$

$$\frac{G}{U^*} = 11.2 + 97.5U^*. \tag{7c}$$

The R^2 values for the above curve-fits are 0.91, 0.98 and 0.93, respectively. Experimental results for some data points, as could be read form the plots in Ref. [17], are also shown on the same chart. Note that the slope shows the form drag coefficient and the y-axis intercept (G/U^* axis) gives μ/K. Using this approach, the permeability for three samples are obtained as 8.2, 12.2, and 17 ($\times 10^{-7}$ m^2) for cases when the plates are 2, 2.6, and 3.2 mm apart, respectively. This leads to $\zeta = 63.3$ (Pa s m^{-2}) regardless of the plate–plate distance despite the fact that the f-phase permeability is tripled when the maximum plate spacing (3 mm) is reached. Note that [17] reported experiments conducted on the same heat exchanger with three different plate spacing being 2, 2.6, and 3.2 mm. The scattered data-points are taken from Figs. (5–7) of [17]. The lines are fitted to these data points and are best described by Eq. (7a–c) above. However, this observation can only be generalized to other cases, where the BDPM is a designed porous medium like the heat exchanger modelled in this study, following further investigation and extension of the results to other geometries. Finally, Fig. 3a is presented to show the dimensionless pressure gradient versus the pore-Reynolds number, with $K^{0.5}$ used as the length scale, for all three cases considered here. In the limit of form-drag dominated flow, the three curves are close to the average form drag coefficient C_F value of 0.13. At $Re_K = 100$, the plots lead to C_F values of about 0.15, 0.134, and 0.136 for samples with 2, 3 and 2.6 mm spacing, respectively. The difference between these C_F values is within the experimental uncertainty of the results reported in Ref. [17]. Therefore, the average C_F is reported here. In the limit, however, as the fluid velocity tends to be too high for the viscous drag to be comparable with the form drag, one expects C_F values of 0.136, 0.122, and 0.127 for the samples according to Eq. (7a–c).

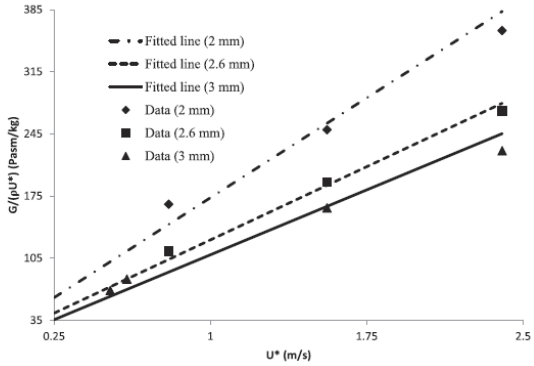

Fig. 2. Pressure drop divided by velocity versus velocity.

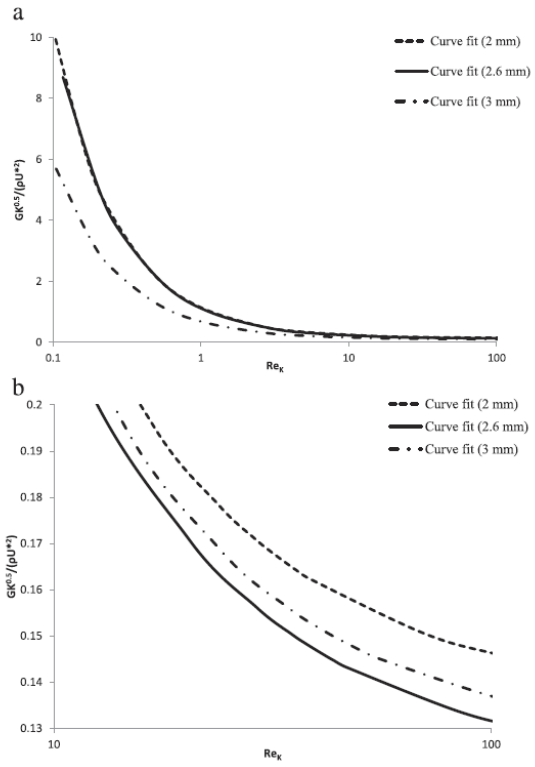

Fig. 3. a) Normalized pressure gradient versus pore-Reynolds number. (b) Zoomed view of (a) for high Re range.

3. Conclusion

Experimental results are used to evaluate the theoretical model developed in Ref. [1] and also to validate the assumptions made therein. In particular, it was noted that, over the range of parameters considered here, both the form drag and the momentum exchange coefficient are homogenous, constant, and velocity-independent. Numerical values are obtained for these two by mapping the experimental data on the theoretical model.